# WET AIR DRYING BY ADSORPTION ON ACTIVE CARBON IMPREGNATED WITH CALCIUM CHLORIDE

Maria SPIRIDON, Marius Sebastian SECULA and Stelian PETRESCU[*]

"Gh. Asachi" Technical University of Iasi, Faculty of Chemical Engineering and Environmental Protection, Department of Chemical Engineering, 71 Bd. D. Mangeron, Iasi, 700050, Romania

In this paper is presented an experimental study of mass transfer at adsorption of water vapours from air on a fixed bed of active carbon grains impregnated with calcium chloride. Experiments were performed at the atmospheric pressure and 38°C using cylindrical grains of active carbon impregnated with calcium chloride as adsorbent, and air as gaseous phase at various values of flow rate and humidity. Adsorption rate, $v_a$, drying degree, $\eta_u$, as well as their time variations, mean adsorption rate, $\overline{v_a}$, and mean apparent mass transfer coefficients ($\overline{K}, \overline{K_v}$) were determined. Based on the obtained results, it is studied the influence of air flow rate and humidity on $v_a$ and $\eta_u$. Further, the results are compared with those obtained at water vapour adsorption on non-impregnated active carbon and silica gel impregnated with calcium chloride and lithium bromide respectively.

## INTRODUCTION

Air has been one of the most used gases in technique and consequently, over time, all the known drying methods have been studied and employed. One of these frequently met techniques consists in the separation of water vapour from air by adsorption, where are used adsorbents such as silica gel, molecular sieves, activated alumina and active carbon.

The necessity of increasing drying process rate of gases by adsorption led to achieving novel adsorbent materials, selective for water vapours. These materials are based on a porous matrix impregnated with a hygroscopic inorganic salt that increases their adsorption capacity. At present, silica gel and activated alumina are used as porous matrices, and calcium chloride, lithium bromide and lithium chloride as inorganic salts.

Literature contains a high number of works approaching the study of kinetics and mass transport at gas adsorption at single particle scale

and in fixed bed of particles.[1-25] Nevertheless, in what concerns air drying on composite materials obtained by impregnation with the above mentioned hygroscopic inorganic salts, only a few papers[9-13] treating aspects related on the equilibrium, kinetic and especially mass transport have been reported. Also, in literature there are reported works[14-23] approaching kinetic and mass transport studies at gas adsorption on active carbon. However, a limited number of papers deal with the study of adsorption of water vapours from air on active carbon.[17-19] Thus, Cossarutto *et al.*[15] and Zimny *et al.*[16] studied equilibrium and kinetic of water vapour adsorption on active carbon. They established the influence of chemical and structural characteristics of active carbon surfaces during adsorption and desorption processes of water vapours. Cristoph and Thorpe[24] investigated the heat transfer and determined the pressure loss through a fixed bed of active carbon at low Reynolds numbers, using inert gases.

[*] Corresponding author: spetresc@ch.tuiasi.ro

The present paper approaches the experimental study of mass transfer at adsorption of water vapours from air on fixed bed of active carbon impregnated with calcium chloride. There are experimentally determined adsorption rate, $v_a$, drying degree, $\eta_u$, as well as their variations in time, mean adsorption rate, $\overline{v_a}$, and mean apparent mass transfer coefficients ($\overline{K}, \overline{K_v}$). The experiments were carried out at the atmospheric pressure and temperature of 38°C using cylindrical grains of active carbon impregnated with calcium chloride as adsorbent, and air as gaseous phase, at various values of flow rate and humidity. Based on the obtained results, it is emphasized the influence

of air flow rate and humidity on $v_a$ and $\eta_u$. Further, the results are compared with those obtained at water vapour adsorption on non-impregnated active carbon and silica gel impregnated with calcium chloride and lithium bromide.

## EXPERIMENTAL

In order to carry out the experimental investigations, it was used a set-up that is represented in Fig. 1. This installation consists in a vertical cylindrical column (1), heat exchanger (2), thermostat (3), air wetting chamber (4), ventilating fan (5), digital technical balance (6), valves for controlling air and water flow rates, and also measuring and control systems for temperature, air flow rate and relative humidity.
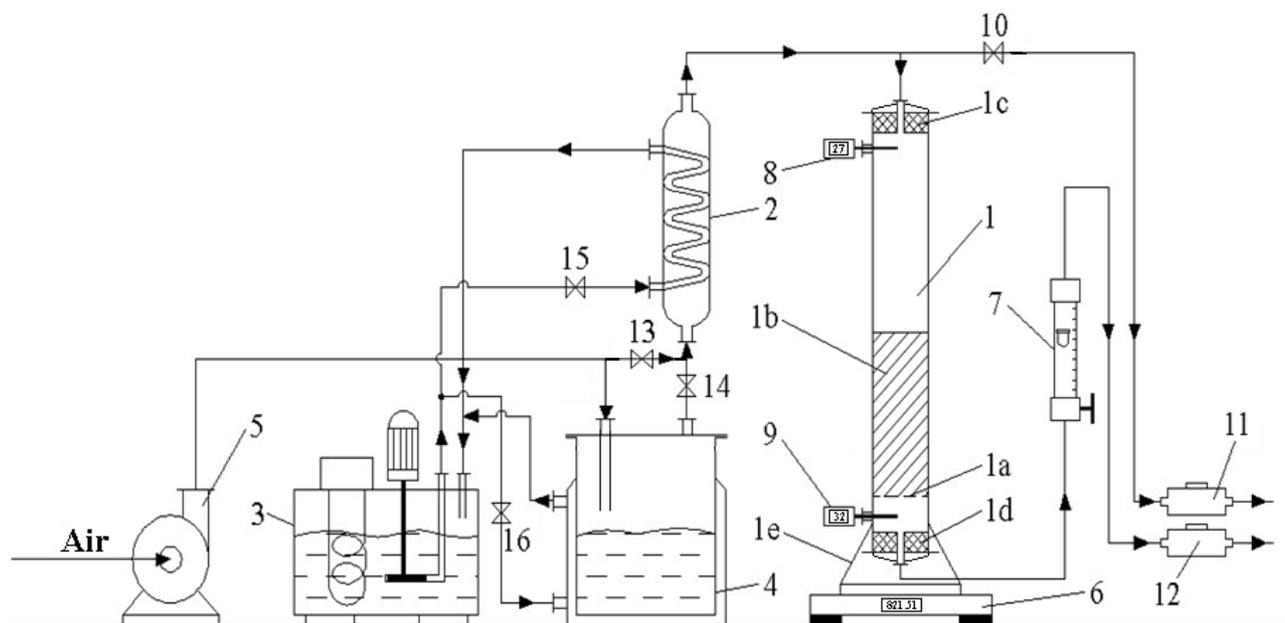


Fig. 1 – Experimental set-up: 1 – adsorption column, 2 – heat exchanger, 3 – thermostat, 4 – air wetting chamber, 5 – ventilator fan, 6 – digital technical balance, 7 – flowmeter, 8, 9 – digital thermometers, 10, 13, 14, 15, 16 – valves, 11, 12 – chambers for psychrometer probes at the input and output of the adsorbed column.

Column (1), having the function of adsorption unit, is made of PVC, and has at both ends lids provided with air inlets and outlets. At the bottom of the adsorption column, a stainless steal sieve (1a) supports the adsorbent bed. In order to seal the column, two rubber rings, (1c) and (1d), were fasten at both ends. The adsorption column is fixed on a metallic support (1e).

For heating the air it was used a heat exchanger (2) that is made of thermoresistant glass. In the inner part, the heat exchanger is provided with a serpentine coil fed with warm water from the thermostat (3). By means of air wetting chamber (4), air humidity can be adjusted to a desired value. Chamber (4) is a cylindrical stainless steal recipe provided with heating jacket through which flows hot water from the thermostat (3). The lid of this recipe is provided with an air inlet and outlet. Air flows through the experimental set-up by means of ventilator fan (5).

The water quantity retained was determined by means of a digital balance having the accuracy of ±0.01 g. The control of gas flow rate was performed by means of flowmeter (7), and the air temperature at the input and output of the bed was measured with digital thermometers (8) and (9).

In order to measure the air humidity at the column input, the installation was provided with a by-pass (valve (10)) and a probe (11) provided with a gauge for the psychrometer thermocouple. Air humidity at the column output was measured with a second psychrometer having its thermocouple fixed in chamber (12). Air temperature and air humidity were fixed by adjusting the position of the valves (13), (14), (15) and (16).

The adsorption process was conducted in a fixed granular bed operated continuously. Geometric parameters of the fixed adsorbent bed are as follows: the height of 0.15 m and diameter of $2.95 \cdot 10^{-2}$ m.

In the experiments were used active carbon (CA) and active carbon impregnated with calcium chloride (MCC1) obtained from cylindrical grains of active carbon having $3.5 \cdot 10^{-3}$ m in diameter and $3.5 \cdot 10^{-3}$ m in height, and aqueous solutions of calcium chloride; calcium chloride content in adsorbent bed is of 12.54 % by weight.

Experimental investigations were performed at the atmospheric pressure and temperature of 38°C using as gaseous phase wet air at two values of the relative humidity: 60 and 85%, and four levels of air flow rate (300, 600 and 1200 L·h$^{-1}$).

For each experiment, the quantity of retained water ($\Delta m$) was determined by measuring the initial weight ($m_0$) of the adsorption column and its momentary weight ($m$) at several moments of time (10, 20… 120 min.). At the same time, by means of a digital psychrometer and thermometer, the evolution of air relative humidity and temperature respectively at the bed output were measured and recorded.

## METHODS

Gas drying is performed by retaining water vapours from gas on a porous adsorbent. In case of gas drying in fixed bed of granular adsorbent, the adsorption rate can be determined with the relationship:

$$v_a = \rho_s \frac{dX}{dt} \qquad (1)$$

Expressed as weight ratio, the mean water concentration in the bed is given by the relationship:

$$X = \frac{\Delta m + m_0 \cdot \overline{x_0}}{m_0 \left(1 - \overline{x_0}\right)} \qquad (2)$$

Drying degree can be calculated with the following relationship:

$$\eta = 1 - \frac{C}{C_0} \qquad (3)$$

The apparent volumetric mass transfer coefficient was determined using the values of the formal adsorption rate:

$$v_a = K_v \left(C - C^*\right)_{mean} \qquad (5)$$

Mean driving force is described by the relationship:

$$\left(C - C^*\right)_{mean} = \frac{\left(C_0 - C_0^*\right) - \left(C - C^*\right)}{\ln \dfrac{C_0 - C_0^*}{C - C^*}} \qquad (6)$$

Mean adsorption rate is defined as:

$$\overline{v_a} = \frac{1}{t} \int_0^t v_a(t)\,dt \qquad (7)$$

Mean apparent volumetric mass transfer coefficient can be calculated using the relationship:

$$\overline{v_a} = \overline{K_v}\left(\frac{C_0 + \overline{C}}{2} - \overline{C^*}\right) \qquad (8)$$

where: $\overline{K_v} = \overline{K} \cdot a_s$ .

## RESULTS AND DISCUSSION

In Fig. 2 is presented the variation of water concentration in MCC1 composite material as a function of time at several values of flow rate and two values of initial relative humidity of air (60%, 85%). Mean water concentration in solid was calculated with equation (2). According to Fig. 2 water concentration in MCC1 (active carbon – calcium chloride) composite material increases in time irrespective of the values of relative humidity and air flow rate. At longer durations of the adsorption process, the increase of water concentration in solid is slower. In solid, the water concentration increases with gas flow rate.

Fig. 3 shows the variation in time of water concentration in MCC1 adsorbent material and CA active carbon, in case of water vapour adsorption in air having relative humidity of 60% and flow rate of 600 L/h. On the same graph are also plotted the adsorption rates in time of other two adsorbent materials: MCS2 and MCSS2. These materials were obtained by impregnating spherical grains (2.57 mm in diameter) and non-spherical grains (2.5 mm in equivalent diameter) of silica gel with lithium bromide resulting in composite materials: MCSS2 and MCS2 respectively. MCSS2 and MCS2 composite adsorbent materials contain 5.97 wt % LiBr and 7.1 wt % LiBr respectively.

It can be noted that MCC1 presents a higher adsorption capacity for water vapours in comparison to the other considered materials: CA, MCS2 and MCSS2.

In Fig. 4 are plotted the time variation curves of temperature at the output of the fixed bed of composite adsorbent material, at two values of gas flow rate (600 and 1200 L/h), for an air relative humidity of 60%. Diagram in Fig. 4 emphasizes that the process takes place under non-adiabatic and non-isothermal regime.
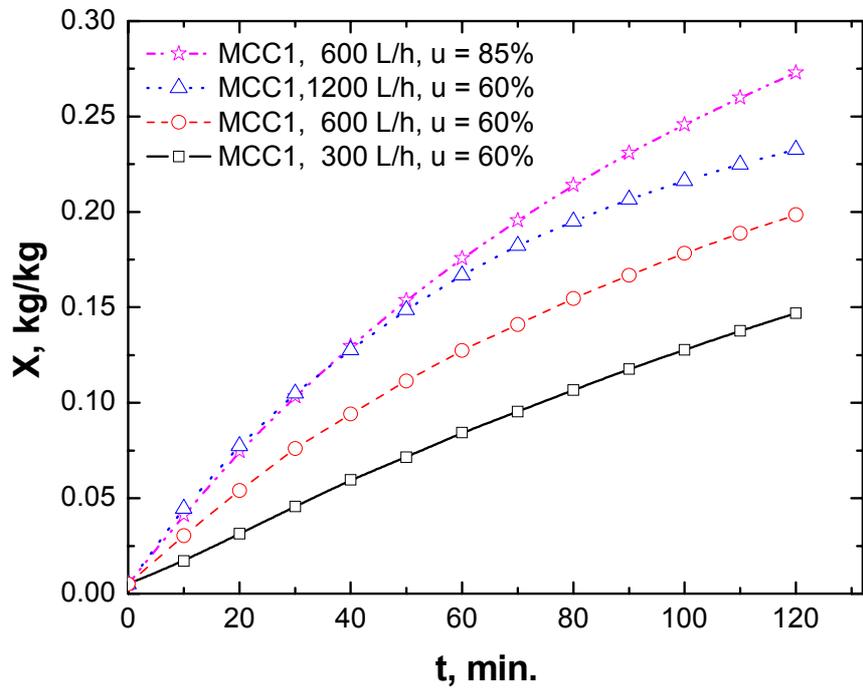
Fig. 2 – Concentration of water in solid adsorbent bed as a function of time at water vapour
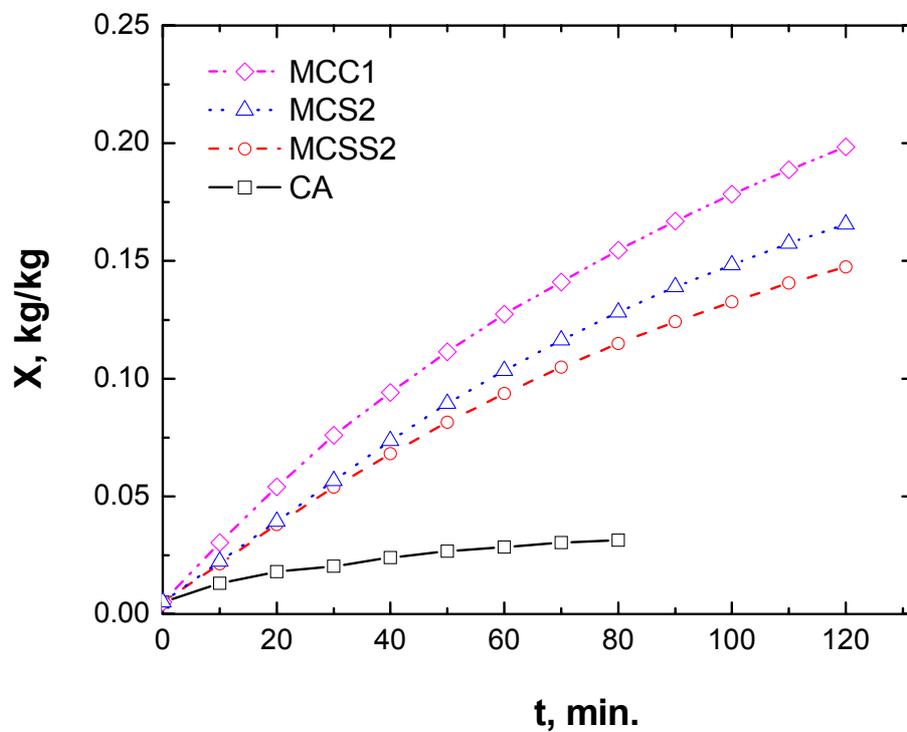adsorption on MCC1 at different values of air flow rate and relative humidity.



Fig. 3 – Concentration of water in solid adsorbent bed as a function of time at water vapour
adsorption on different adsorbent materials at an air flow rate of 600 L/h and an air relative humidity of 60%.
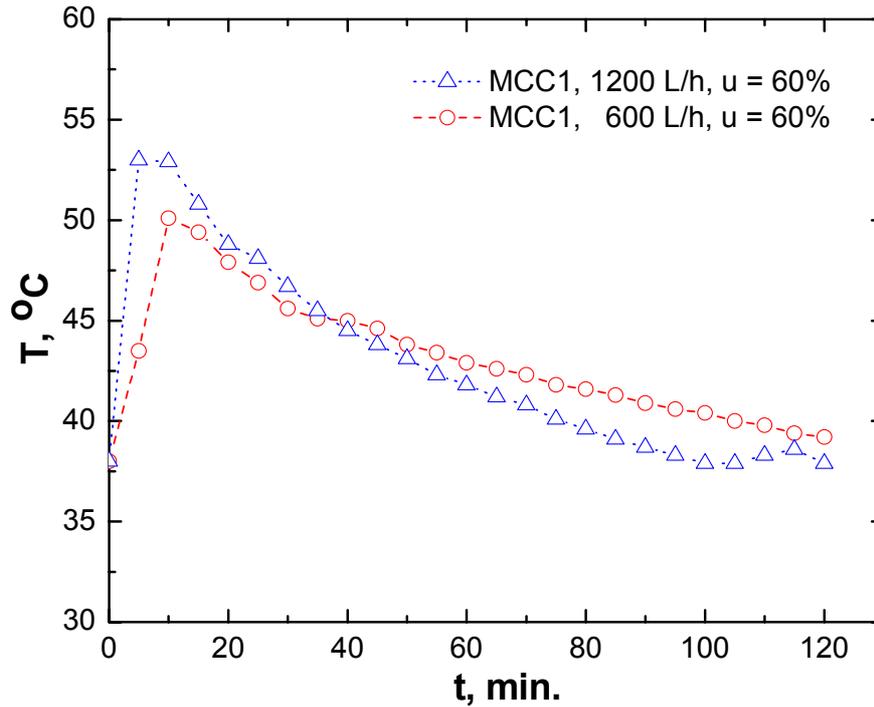
Fig. 4 – Temperature at the output of adsorbent bed vs. time at water vapour adsorption on MCC1
at two values of air flow rate and a 60% relative humidity of air.

Based on the experimental values of air relative humidity at the output of adsorbent fixed bed, it was established the variation in time of water vapours concentration in gaseous phase. The obtained results are plotted in Fig. 5. It can be noted an increase in time of water vapour concentration at the bed output, this concentration tending at longer durations (more than 120 min.) to the initial value $C_0$. Obviously, the higher the air flow rate, the bigger the concentration C is, and the time required to reach value $C_0$ is lower.
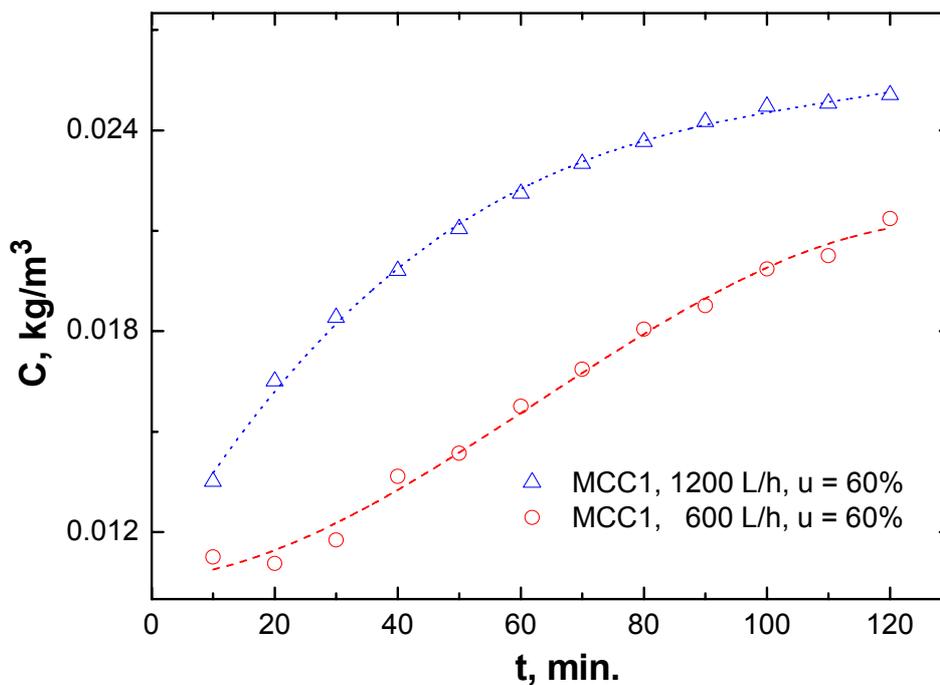


Fig. 5 – Variation in time of water vapour concentration in air using MCC1 at two values of air
flow rate and an air relative humidity of 60%.

Using relation (1) and the results previously achieved, the adsorption rate, $v_a$, was determined, which is in fact the specific mass flux per unit volume of adsorbent. From Fig. 6 it follows that the adsorption rate decreases in time for each value of gas flow rate. This fact is due to a diminished driving force of the adsorption process in time as a consequence of an increase of the equilibrium concentration of water vapours in gaseous phase ($C^*$). Equilibrium concentration $C^*$ is influenced by temperature and water concentration in adsorbent material. As water concentration in adsorbent grows, while temperature decreases in time, these will lead to an increase of equilibrium concentration $C^*$.

Gaseous phase flow rate and air relative humidity at the input influence positively the adsorption rate, which means that increasing air flow rate and relative humidity leads to an increase of adsorption rate.

Fig. 7 shows the time variation of water adsorption rate from air on MCC1 and CA materials for an air relative humidity of 60% and an air flow rate of 600 L/h, comparative to the variation in time of adsorption rate on MCS2 and MCSS2 materials, under similar conditions. As can be noticed, the adsorption rate of water vapours on MCC1 is comparable with those corresponding to

MCS2 and MCSS2, and is much higher than in case of active carbon.

Using equation (4), it was calculated the drying degree of air. The obtained values are presented in Fig. 8. As can be seen, drying degree becomes lower in time due to the gradual saturation of the MCC1-adsorbent bed, which determines an increase in time of water vapour concentration in air. Drying degree values closer to unity could be reached by employing more adsorption steps with intermediary cooling.

Based on data obtained for adsorption rate and equations (7) and (8), it was determined the mean adsorption rate and mean apparent mass transfer coefficient. Apparent mass transfer coefficients characterize the intensity of gas drying process by adsorption and resistance to transfer. $1/\overline{Kv}$ or $1/\overline{K}$ represent the overall mass transfer resistance that is equal to the sum of the two individual resistances, namely, external resistance (to transfer through gas phase) and internal resistance (to transfer through the solid material pores). Equilibrium concentrations, $\overline{C^*}$, for the system MCC1-wet air were considered from literature[26] and are presented in Table 1. Values of concentration $\overline{C^*}$ were interpolated at time-averaged values of water concentration in solid phase and temperature.
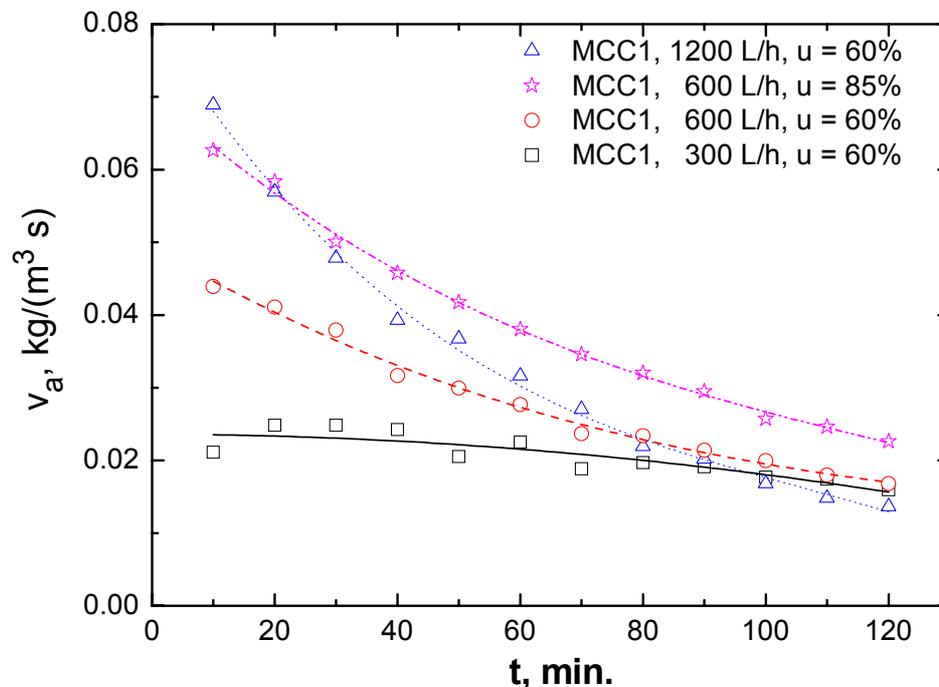


Fig. 6 – Variation of adsorption rate in. time at air-drying by adsorption on MCC1
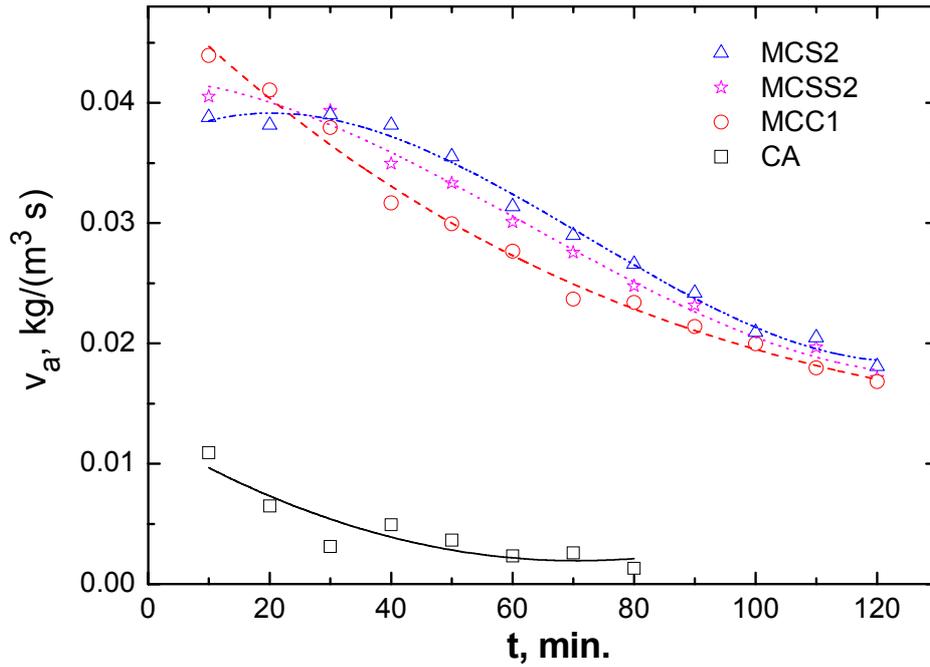at different values of air flow rate and relative humidity.

Fig. 7 – Variation of adsorption rate in. time for the studied adsorbent materials
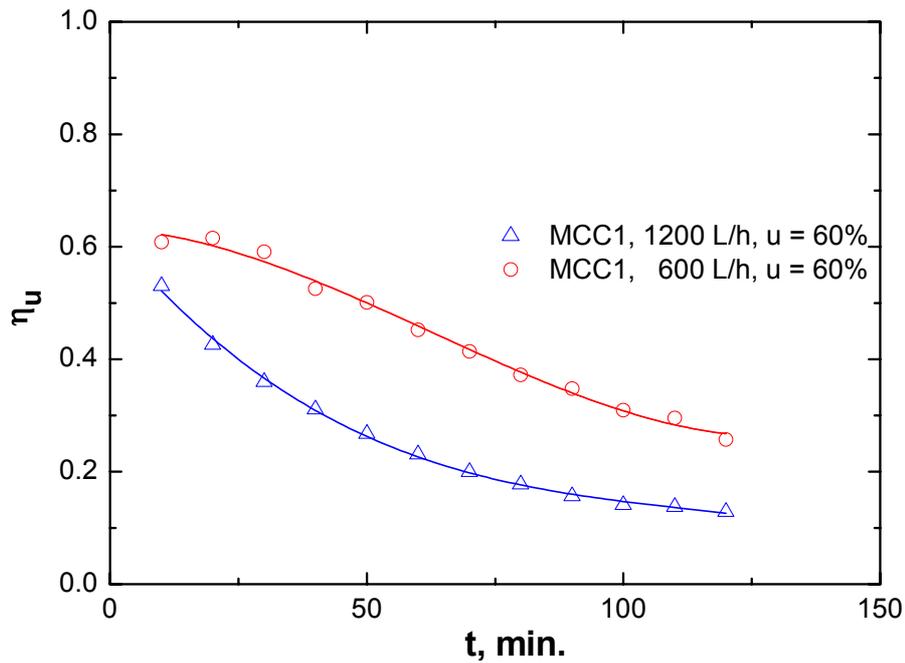at an air flow rate of 600 L/h and an air relative humidity of 60%.



Fig. 8 – Evolution in time of air drying degree obtained on the fixed bed
of MCC1 at two values of air flow rate and an air relative humidity of 60%.

*Table 1*

Equilibrium data

| Material | MCC1 (40.5ºC, 0.076 kg/kg) | MCC1 (41.1ºC, 0.1015 kg/kg) | MCC1 (42.2ºC, 0.1188 kg/kg) | MCC1 (42.8ºC, 0.1389 kg/kg) | MCSS2 (41.2ºC, 0.07635 kg/kg) | MCS2 (41.6ºC, 0.08528 kg/kg) | CA (38.8ºC, 0.01817 kg/kg) |
|---|---|---|---|---|---|---|---|
| $C^*$, kg/m$^3$ | 0.01444 | 0.01928 | 0.02257 | 0.03057 | 0.01468 | 0.0147 | 0.006489 |

Values obtained for the mean adsorption rate and mean apparent mass transfer coefficient, $\overline{K}$, were plotted in Figs. 9 and 10. As can be noted in Fig. 10, air flow rate influences positively mass transfer coefficient. Values obtained experimentally for mass transfer coefficient, $\overline{K_v}$, in case of MCC1 and CA materials were compared to those obtained for other adsorbent materials, such as MCS2 and MCSS2. In Table 2 are presented the values of mean apparent mass transfer coefficient, $\overline{K_v}$, for MCC1, CA, MCSS2 and MCS2 materials. As can be noted, the highest values for mass transfer coefficient are obtained when using MCC1 adsorbent; moreover, these values are much higher than in case of CA adsorbent.
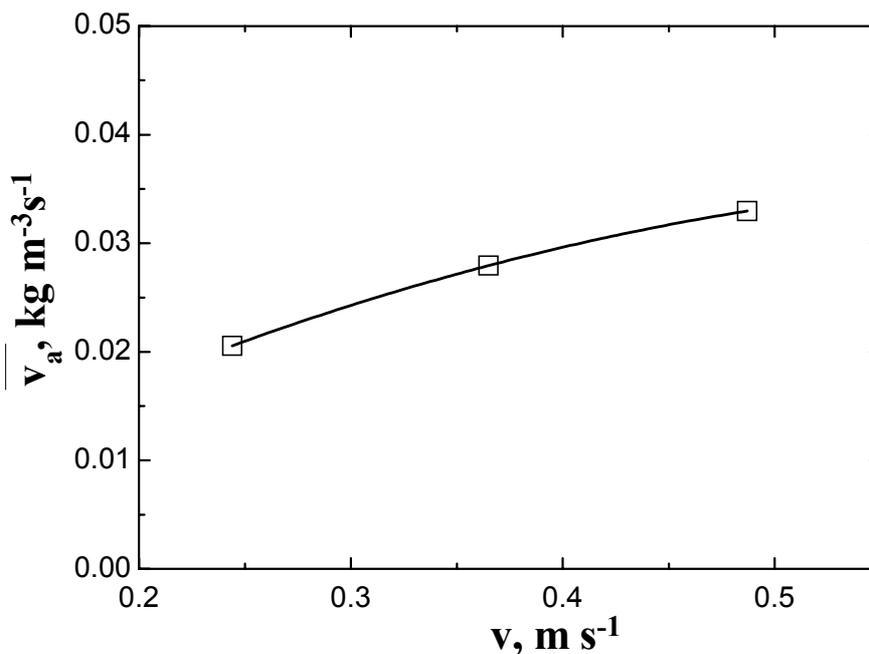


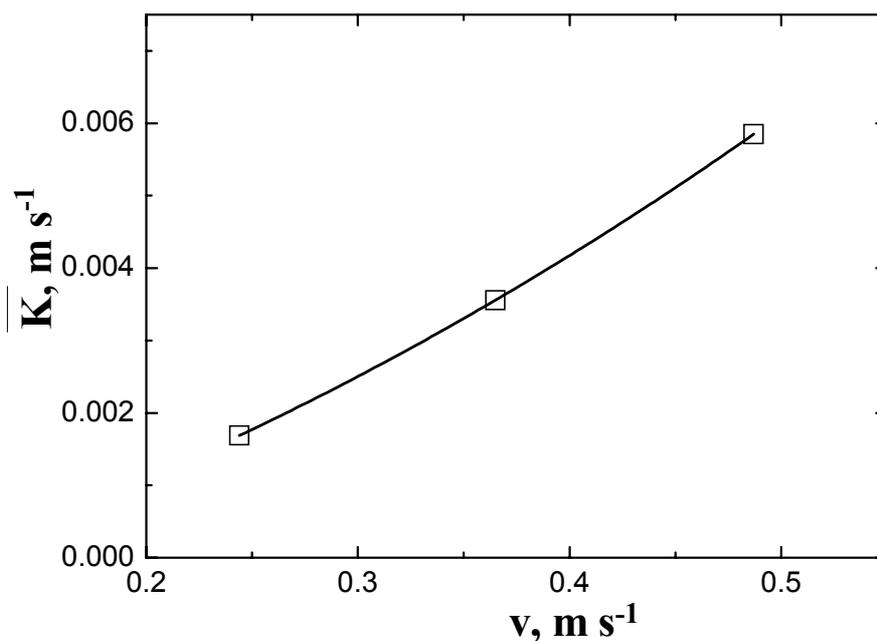Fig. 9 – Dependence of mean adsorption rate on air flow velocity.



Fig. 10 – Variation of apparent mass transfer coefficient with air flow velocity.

*Table 2*

Values of apparent mass transfer coefficient, $\overline{K_v}$, at water vapour adsorption on various materials

| Material | MCC1 | | | | CA | MCSS2 | MCS2 |
|---|---|---|---|---|---|---|---|
| u, % | 60 | 60 | 60 | 85 | 60 | 60 | 60 |
| $M_v$, L/h | 300 | 600 | 1200 | 600 | 600 | 600 | 600 |
| $\overline{K_v}$, s$^{-1}$ | 2.892 | 6.100 | 10.027 | 9.486 | 0.206 | 3.794 | 4.189 |

## CONCLUSION

An experimental study of mass transfer at air drying by adsorption on a novel granular composite material (MCC1) in fixed bed was presented in this paper. The novel material was obtained by impregnating active carbon with calcium chloride.

Using MCC1 (12.54% CaCl$_2$) and active carbon adsorbent materials, there were experimentally determined at atmospheric pressure and 38°C the variations in time of mean water concentration in the bed of adsorbed material, temperature and water vapour concentration in air at the adsorbent bed output.

Based on the primary data obtained experimentally, the adsorption rate of water vapours, drying degree, mean adsorption rate and mean apparent mass transfer coefficients were determined. The obtained results emphasize a positive influence of air flow rate and relative humidity over adsorption rate. On the contrary, air flow rate and relative humidity influence negatively the drying degree.

Also, the obtained results show that the MCC1 composite material presents an adsorption capacity comparable to other adsorbent materials, such as spherical or non-spherical silica gel impregnated with lithium bromide, and much higher than that of active carbon.

## ABBREVIATIONS

$a_S$ − particles specific area, m$^2$·m$^{-3}$;
$C_0$, $C$ − water vapour concentration in gaseous phase at the inlet and respectively outlet of the adsorbent bed, kg·m$^{-3}$;
$\overline{C}$ − time-averaged concentration of water vapours in air at the output of the bed, kg·m$^{-3}$;
$C_0^*, C^*$ − equilibrium concentration of water vapour in gaseous phase at the inlet and respectively outlet of the adsorbent bed, kg·m$^{-3}$;
$\overline{C^*}$ − equilibrium concentration of water vapour in gaseous phase at $\overline{T}$ and $\overline{X}$, kg·m$^{-3}$;

$K$ − apparent mass transfer coefficient, m·s$^{-1}$;
$K_v$ − apparent volumetric mass transfer coefficient, s$^{-1}$;
$\overline{K}$ − mean apparent mass transfer coefficient, m·s$^{-1}$;
$\overline{K_v}$ − mean apparent volumetric mass transfer coefficient, s$^{-1}$;
$m_0$, $m$ − mass of adsorbent bed at t = 0 and t = t respectively, kg;
$M_v$ − gas phase (air) flow rate, m$^3$·s$^{-1}$;
$t$ − time, s;
$T$ − gaseous phase temperature at the output of the bed, °C;
$\overline{T}$ − time-averaged temperature at the output of the bed, °C;
$u$ − air relative humidity, %;
$v_a$ − formal adsorption rate of water vapour, water vapour flux per volume unit of adsorbent, kg·m$^{-3}$·s$^{-1}$;
$X$ − water concentration in adsorbent weight, ratio of water to adsorbent, kg·kg$^{-1}$;
$\overline{X}$ - time-averaged concentration of water in solid phase, kg·kg$^{-1}$;
$x_0$ − water weight ratio in adsorbent at t = 0, dimensionless;
$\Delta m$ − mass variation of adsorbent bed, kg;
$\eta_u$ − drying degree, non-dimensional;
$\rho_s$ − adsorbent particle density, kg·m$^{-3}$.

## REFERENCES

1.  D.M. Ruthven, *Principles of adsorption and adsorption process*, J. Wiley, New York, 1984.
2.  J.M. Coulson and J.F. Richardson, *Chemical Engineering*. Vol. 2, Pergamon Press, Oxford, 1993.
3.  E. Bratu, *Unit Operations in Chemical Engineering*. Vol. 3, Technical Press, Bucharest, 1984.
4.  G. Bozga and O. Muntean, *Chemical Reactors*. Vol. 2, Technical Press, Bucharest, 2001.

5.  O. Floarea and R. Dima, *Mass Transfer Processes and Specific Units*, Didactic and Pedagogical Press, Bucharest, 1986.
6.  T. Dobre and J.G. Sanchez Marcano, *Chemical Engineering Modelling*, Simulation and Similitude, J. Wiley, New York, 2007.
7.  J. Toth, *Adsorption*, M. Dekker, New Jersey, 2002.
8.  S. Motoyuki, *Adsorption Engineering*, Elsevier, Amsterdam, 1990.
9.  B. Dawoud and Y. Aristov, *Int. J. Heat Mass Transfer*, **2003**, *46*, 273-281.
10. Y. Aristov, G. Restuccia, G. Cacciola and V.N. Panon, *Appl. Therm. Eng.*, **200**2, *22*, 191-204.
11. M. Tokarev, L. Gordeeva, V. Romannikov, I. Glaznev and Y.I. Aristov, *Int. J. Therm. Sci.*, **2002**, *41*, 470-474.
12. X.J. Zhang, K. Sumathy, Y.J. Dai and R.Z. Wang, *Int. J. Energy Res.*, **2005**, *29*, 37-51.
13. X.J., Zhang and L.M. Qiu, *Energ. Convers. Manag.*, **2007**, *48*, 320-326.
14. B. Guo, L. Chang and K. Xie, *J. Natural Gas Chem.*, **2006**, *15*, 223-229.
15. L. Cossarutto, I. Zimny, J. Kaczmarczyk, T. Siemieniewska, J. Bimer and J.W. Weber, *Carbon*, **2001**, *39*, 2339-2346.
16. T. Zimny, G. Finqueneisel, L. Cossarutto and J.W. Weber, *J. Colloid Interf. Sci.*, **2005**, *285*, 56-60.
17. D.D. Do and H.D. Do, *Carbon*, **2000**, *38*, 367-373.
18. T.J. Bandosz, B. Buczek, T. Grzybek and J. Jagiello, *Fuel*, **1997**, *76*, 1409-1416.
19. E. Biron and M.J.B. Evans, *Carbon*, **1998**, *36*, 1191-1197.
20. G.O. Wood, *Carbon*, **2002**, *40*, 1883-1890.
21. G.O. Wood, *Carbon*, **1993**, *31*, 195-200.
22. A. Lavanchy and F. Stoeckli, *Carbon*, **1997**, *35*, 1573-1579.
23. C.C. Rodrigues, D. de Moraes Jr., S.W. da Nobrega and M.G. Barbroza, *Biores. Tech.*, **2007**, *98*, 886-891.
24. R. E. Cristoph and R. Thorpe, *Appl. Therm. Emg.*, **1996**, *16*, 419-427.
25. P. Lodewyckx and E.F. Vansant, *Am. Ind. Hyg. Assoc. J.*, **2000**, *61*, 501-505.
26. I. Mămăligă, C. Baciu and S. Petrescu, *Environ. Eng. Manag. J.*, **2009**, *8*, 91-97.